Journal of the Geological Society, *London*, Vol. **161**, 2004, pp. 959–968. Printed in Great Britain.

Isotopic signals from late Jurassic–early Cretaceous (Volgian–Valanginian) sub-Arctic belemnites, Yatria River, Western Siberia

G. D. PRICE[1] & J. MUTTERLOSE[2]

[1]*School of Earth, Ocean and Environmental Sciences, University of Plymouth, Drake Circus, Plymouth PL4 8AA, UK (e-mail: g.price@plymouth.ac.uk)*

[2]*Institut für Geologie, Mineralogie und Geophysik, Ruhr-Universität Bochum, Universitätsstrasse 150, D-44801, Bochum, Germany*

Abstract: This contribution presents the first detailed oxygen and carbon isotope record from the latest Jurassic–early Cretaceous interval of the Yatria River, subpolar Urals, Siberia. Isotopic compositions have been determined on well-preserved belemnite samples from the genera *Lagonibelus*, *Cylindroteuthis* and *Acroteuthis*. These new data indicate a shift to lower temperatures from the late Volgian into the late Valanginian, with some warmer phases recognized within the Ryazanian and earliest Valanginian. The lowest temperatures of the late Valanginian, consistent with subfreezing polar temperatures, are coincident with an inferred eustatic sea-level fall. A late Valanginian positive shift in carbon isotopes correlates with the carbon isotope excursion recorded from Tethyan successions. The most positive carbon isotope values correspond to the most positive oxygen isotope values (and hence lowest palaeotemperatures). In the absence of widespread Valanginian organic-rich black shale deposition, the carbon isotope excursion may point to increased storage of organic carbon in coastal areas and/or enhanced preservation within stratified waters in high-latitude basins. At these higher latitudes, where rates of weathering were presumably much lower because of the prevalent cold climate, the isotopic data may point to pulses of productivity being brought about by increased riverine nutrient transfer and also by nutrients being released by the melting of ice. The correlation between positive carbon isotopes and cool climates may indicate the effectiveness of these high-latitude carbon sinks and their ability to draw down atmospheric CO_2, resulting in an ‘inverse greenhouse’ effect.

Keywords: Jurassic, Valanginian, Siberia, belemnites, stable isotopes.

Subfreezing polar temperatures during the Jurassic and Cretaceous are considered incompatible with widely accepted palaeoclimate data. This period is commonly viewed as a time of warm global climates with a low global temperature gradient, giving rise to weakly defined climatic zonation and warm polar regions (e.g. Frakes 1979; Hallam 1993). Particularly compelling evidence for polar warmth is provided by physiognomic analysis of mid- and late Cretaceous floras from Alaska and northeastern Asia (e.g. Herman & Spicer 1997) and has also been provided by oxygen isotope derived temperature determinations (e.g. Pirrie & Marshall 1990; Huber 1998).

A feature of the early Cretaceous is a series of positive carbon isotope excursions (e.g. the late Valanginian) identified within Tethyan and Atlantic areas (e.g. Lini *et al*. 1992; Wortmann & Weissert 2001) and also from sediments from the Pacific Ocean (e.g. Bartolini 2003). Positive carbon isotope excursions within the early Cretaceous have been attributed to greenhouse climate conditions (e.g. Lini *et al*. 1992; Föllmi *et al*. 1994; Weissert *et al*. 1998). A number of palaeoclimatological studies (e.g. Kemper 1987; Frakes & Francis 1988; Weissert & Lini 1991; Price 1999; Alley & Frakes 2003) indicate at least seasonally low ocean temperatures and the possibility of limited polar ice during the early Cretaceous. Such data are, however, not widely distributed in the Cretaceous (Bennett & Doyle 1996; Price 1999) and hence other palaeoproxies are required to lend support to glacial phases in a Jurassic–Cretaceous greenhouse Earth.

A number of workers, including Ditchfield (1997) and Pucéat *et al*. (2003), have postulated, on the basis of oxygen isotopic analyses, that seasonally low ocean temperatures and limited polar ice caps were present within the early Cretaceous. Decreases in carbon isotope values from the marine record across the Jurassic–Cretaceous boundary (e.g. Weissert 1989; Weissert & Mohr 1996; Ruffell *et al*. 2002) have also been interpreted as evidence of a transition from a warm and humid greenhouse climate to increasing aridity and possibly cooler conditions within the earliest Cretaceous. These published marine isotope records have often been constructed from outcrop exposures within Europe using a composite of different localities with varying diagenetic histories and sometimes poor sample resolution. This contribution presents a late Jurassic (Volgian)– early Cretaceous (early Hauterivian) carbonate (belemnite) isotope record from Western Siberia. A number of studies (e.g. Pirrie & Marshall 1990; Ditchfield 1997; Podlaha *et al*. 1998; Price *et al*. 2000; van de Schootbrugge *et al*. 2000) have demonstrated that, with appropriate constraints placed upon the isotopic composition of seawater, credible palaeotemperature trends can be derived from the isotopic analysis of belemnites. With respect to the early Cretaceous, isotopic data are derived largely from mid- to low latitudes and may therefore not necessarily reflect ambient climatic conditions at higher latitudes. Hence our understanding of Cretaceous climate has been hampered by a lack of data from northern high latitudes. It is the purpose of this contribution to provide robust, biostratigraphically constrained, oxygen and carbon isotopic data from high latitudes that contribute to the debate on whether the early Cretaceous was at times characterized by sub-freezing polar temperatures. A concurrent analysis of the belemnite fauna will also be undertaken to provide important information regarding the palaeoecological and palaeoceanographic setting.

Geological setting

Samples were obtained from the Yatria River, exposed on the eastern slope of the sub-Arctic Ural Mountains (Fig. 1a). Two sections were examined: Location One is 30 km south and Location Two *c*. 20 km south of the village of Saranpaul (Fig. 1b). At Location One, 80 m of sediments of late Volgian, Ryazanian, Valanginian and early Hauterivian age were examined (Fig. 3). The lowermost 6 m consist of dark grey–green glauconitic sands. This unit has been assigned to the *Kachpurites fulgens* and *Craspedites subditus* ammonite zones (Golbert *et al*. 1975) and is hence late Volgian in age. Above these sands is a 3.8 m thick unit of gravelly sands, with phosphatic concretions occurring at the base. This unit contains numerous fragments of bivalve shells, internal moulds of ammonites and abundant belemnites. Based upon the ammonite fauna (Golbert *et al*. 1975) this unit has been assigned to the early Ryazanian, *Hectoceras kochi* ammonite zone. Overlying, the *Surites analogus* and *Tollia payeri* ammonite zones are recognized, followed by the Valanginian *Temnoptychites insolutus*, *Polyptychus michalskii* and *Dichotomites ramulosus* ammonite zones. The uppermost part of the succession can be correlated with the early Hauterivian *Homolsmites bojarkensis* and *Speetoniceras versicolor* ammonite zones (Golbert *et al*. 1975). An early Cretaceous (Ryazanian–Hauterivian) age for these units has been confirmed by dinoflagellate cyst investigations of the Yatria section (e.g. Lebedeva & Nikitenko 1999).

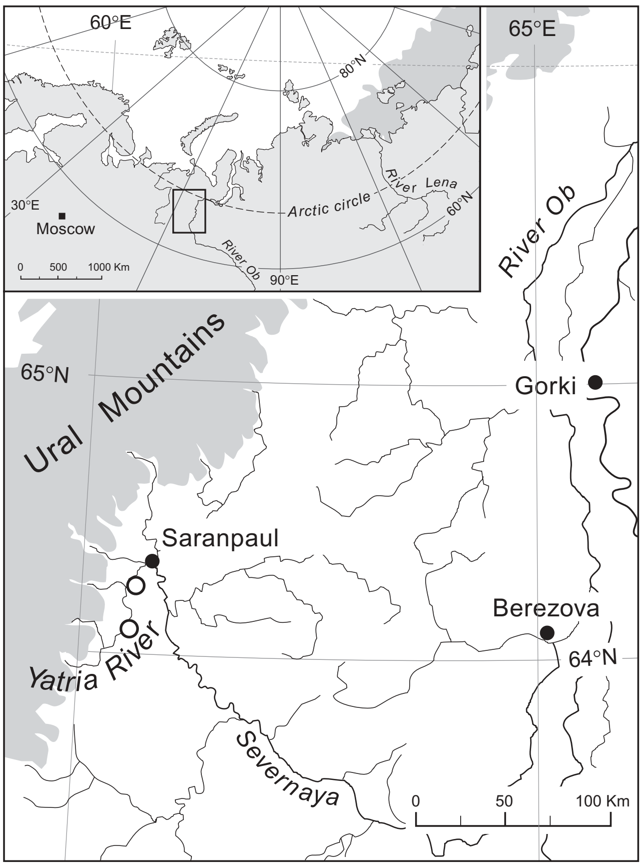

Fig. 1. The Yatria River sections on the eastern slope of the sub-Arctic Ural Mountains (Western Siberia), 20 and 30 km south of the village of Saranpaul.

At Location Two, 23 m of sediments of early Valanginian–early Hauterivian age are exposed (Fig. 4). The age assignment of this succession is also based upon the recognition of the *P. michalskii*, *D. ramulosus*, *H. bojarkensis* and *S. versicolor* ammonite zones (Golbert *et al*. 1975). This zonal scheme may be correlated with both standard Boreal (e.g. Zakharov *et al*. 1997) and Mediterranean (e.g. Hoedemaeker 1990; Hoedemaeker & Rawson 2000) time scales. For example, the Valanginian *P. michalskii* ammonite zone is correlatable with the *Busnardoites campylotoxus* zone, and the *D. ramulosus* zone is the equivalent of the *Saynoceras verrucosum*–*Himantoceras trinodosum* ammonite zones (see Sahagian *et al*. 1996; Baraboshkin 2002). Although the biostratigraphical data indicate a complete succession from the Ryazanian to lowermost Hauterivian, the exposure of the Lower Valanginian succession at Location One was particularly poor.

In the late Jurassic (latest Kimmeridgian–early Volgian) within Western Siberia, a major subsidence episode coincided with a eustatic highstand that induced an extensive marine transgression (Haq *et al*. 1987; Sahagian *et al*. 1996; Pinous *et al*. 1999). The large deep-marine basin covered an area of more than 2×10^6 km^2 (Krylov & Korzh 1984; Gavshyn & Zakharov 1996). The outcrops examined in this study were located, during the earliest Cretaceous, on the western margin of this epicontinental marine basin (Fig. 2) at a palaeolatitude of *c*. 60–65°N (see Smith *et al*. 1994; Pinous *et al*. 2001). This area was separated from the Moscow and Pechora basins by the (palaeo) Urals and formed a southern extension of the Boreal–Arctic sea (Baraboshkin *et al*. 2003), but without any direct connection with seaways towards the Tethys in the south. The accommodation that developed during the late Jurassic was subsequently filled during the early Cretaceous regression. Sediment supply rates

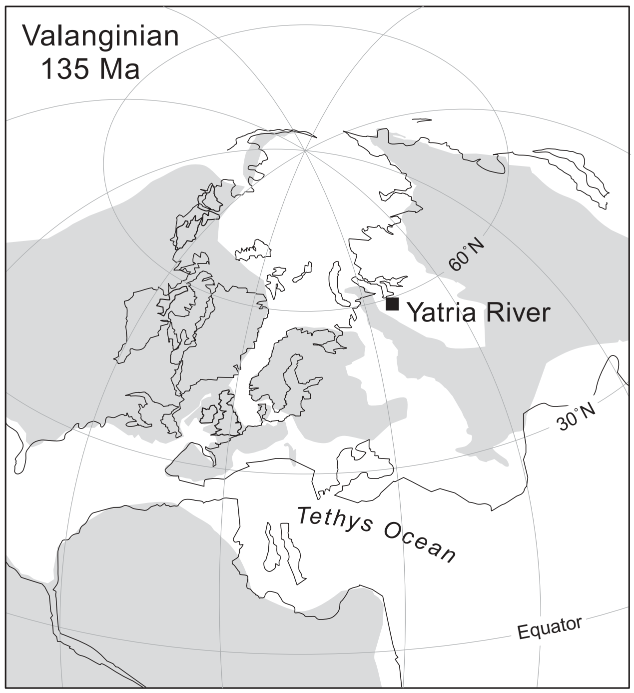

Fig. 2. The palaeogeographical setting of Europe and Western Siberia during Valanginian times (modified from Smith *et al*. (1994) and Baraboshkin (2002)), showing the position of the Yatria River outcrops located on the western margin of a large epicontinental marine basin, a southern extension of the Boreal–Arctic sea.

dramatically increased during the Ryazanian and were supplied from the East Siberian Highlands and the Urals (Pinous *et al*. 2001). Within the Yatria River area these marine units, of early Cretaceous age, are overlain by continental strata deposited in coastal plain environments such as lagoons and lakes (Golbert *et al*. 1975; Lebedeva & Nikitenko 1999).

The latest Jurassic–earliest Cretaceous is also marked by a distinctive provincialism of marine biota. In the northern hemisphere, marine floras and faunas show a clear differentiation into two realms, Tethyan and Boreal. The Boreal Realm includes strata in Russia, northern Europe, Greenland and Alaska. The palaeobiogeographical patterns have been well documented for various groups of marine organisms, in particular for calcareous nannofossils (Mutterlose 1992; Mutterlose & Kessels 2000; Street & Bown 2000), brachiopods (Michalik 1992), ammonites (Hoedemaeker 1990; Rawson 1994), belemnites (Doyle 1987; Mutterlose 1988) and bivalves (Dhondt 1992). Endemic marine biota are typical for this interval; the restricted epicontinental seas favoured *in situ* evolution of benthonic, planktonic and nektonic organisms. The evolution of endemic boreal ammonite taxa started in the mid- to late Jurassic and peaked in earliest Cretaceous (Berriasian) times. This palaeobiogeographical differentiation is reflected in the use of two different stage names for the interval covering the Jurassic–Cretaceous boundary interval: in the Tethyan Realm the stage names Tithonian and Berriasian are used, whereas in the Boreal Realm the terms Volgian and Ryazanian are employed.

Methods

A total of 300 Volgian–Hauterivian belemnite rostra were collected bed-by-bed from the two locations examined and subsequently analysed (Figs 3 and 4). Where possible, multiple samples were collected from the same stratigraphic horizon. The preservation of the belemnite rostra has been assessed through trace element and stable isotopic analyses, backscattered scanning electron microscopy (BSEM) and carbonate staining (following the technique of Dickson (1966)). Prior to chemical and isotopic analysis, areas most susceptible to diagenetic alteration as indicated by carbonate staining (typically the exterior of each rostrum and the apical line) were removed by drilling. The remains were fragmented (to sub-millimetre size), washed in pure water, and dried in a clean environment. Fragments were subsequently picked under the binocular microscope to secure those judged to be best preserved, and were then analysed for oxygen and carbon isotopes. Subsamples for chemical analysis (Mg, Sr, Fe, Mn) were dissolved in concentrated hydrochloric acid and analysed by inductively coupled plasma–atomic emission spectrometry using a Varian 200 system. Based upon analysis of duplicate samples, reproducibility was better than ±3% of the measured concentration of each element.

Stable isotope data ($\delta^{18}O$ and $\delta^{13}C$) were generated on a Finnigan MAT 251 mass spectrometer coupled to the Carbo Kiel online carbonate preparation line at the Leibniz-Laboratory for Radiometric Dating and Stable Isotope Research, Kiel, Germany. These data are given in δ notation with respect to the V-PDB standard. Replicate analyses of standards, for both $\delta^{18}O$ and $\delta^{13}C$, gave a reproducibility generally better than 0.1‰. All analytical data derived from the belemnites (O and C isotopes, Sr, Mg, Mn, Fe and trace elements) can be obtained from the Society Library or the British Library Document Supply Centre, Boston Spa, Wetherby, West Yorkshire LS23 7BQ, UK as Supplementary Publication No. SUP 18210 (10 pages). It is also available online at http://www.geolsoc.org.uk/SUP018210.

Results

The belemnites sampled in this study were mostly translucent and retained the primary concentric banding that characterizes belemnite rostra. A few samples exhibited particularly prevalent areas of endolithic borings around the margins of the rostra. Individual borings were subsequently infilled with calcite spar or fine-grained detrital material. Carbonate staining and BSEM analysis indicated that these areas tended to be Fe-rich and also revealed partial replacement by pyrite preferentially along the outermost concentric growth bands. Areas such as these were either removed before subsampling or avoided. Because, as noted above, even subtle diagenetic alteration can potentially destroy any primary isotopic signal, both Mn and Fe concentrations of the belemnites were determined to provide a further means to verify their state of preservation. Relatively low Mn (<100 ppm) and Fe (<150 ppm) concentrations have been measured from modern molluscs and can be assumed to reflect well-preserved shell material (e.g. Pirrie & Marshall 1990; Podlaha *et al*. 1998).

The determined elemental abundances of belemnite rostra

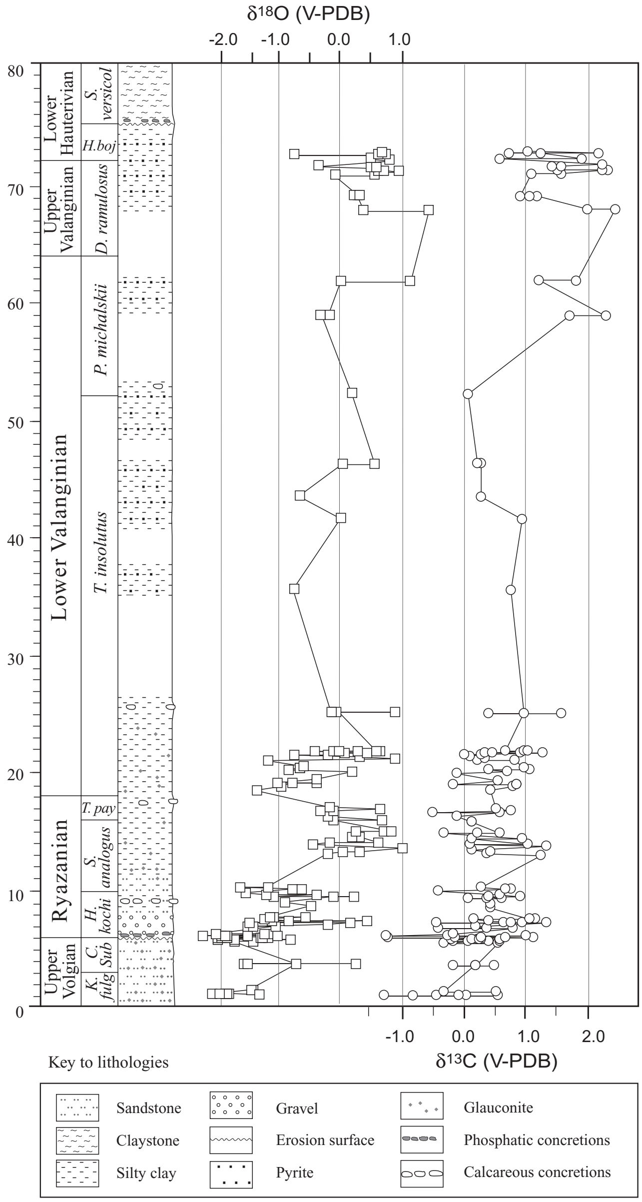

Fig. 3. Sedimentary log from Location One, Yatria River, showing the $\delta^{18}O$ and $\delta^{13}C$ stratigraphy. Biostratigraphical and lithological data from Golbert *et al*. (1975).

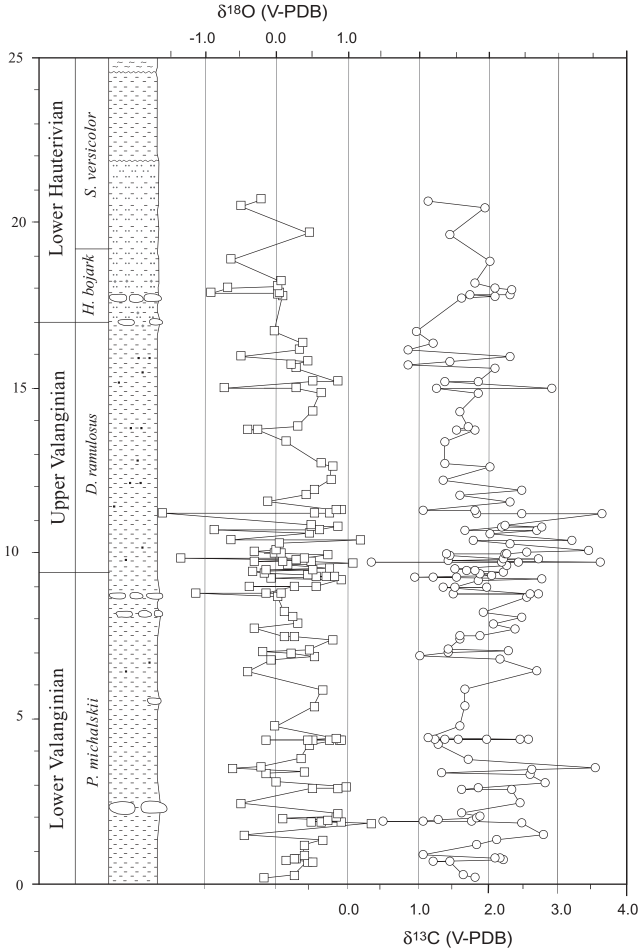

Fig. 4. Sedimentary log from Location Two, Yatria River, showing the $\delta^{18}O$ and $\delta^{13}C$ stratigraphy. Biostratigraphical and lithological data from Golbert *et al*. (1975).

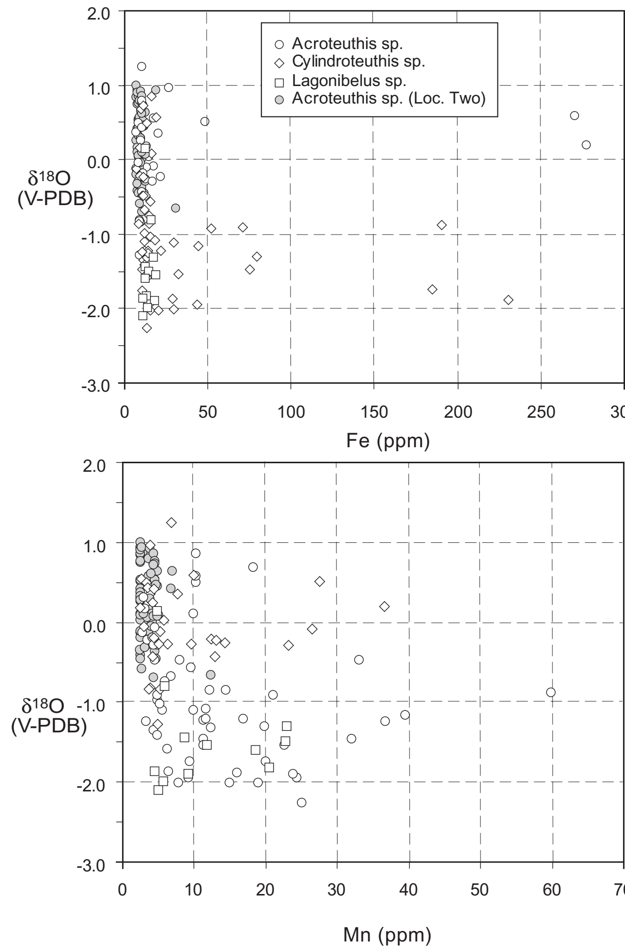

Fig. 5. Cross-plot of $\delta^{18}O$ v. Fe and Mn data derived from belemnite samples of the Yatria River

from Location One were as follows: Sr 358–1607 ppm, mean 1205 ppm; Mn 2–60 ppm, mean 10 ppm; Mg 333–2238 ppm, mean 806 ppm; Fe 3–278 ppm, mean 24 ppm. Abundances for rostra from Location Two were: Sr 775–1758 ppm, mean 1166 ppm; Mn 2–16 ppm, mean 6 ppm; Mg 253–937 ppm, mean 486 ppm; Fe 3–31 ppm, mean 6 ppm. Low Mn (<100 ppm) and Fe (<150 ppm) values are recorded for most of the belemnites. Trace element data (Mn and Fe) were plotted v. $\delta^{18}O$ to constrain any diagenetic alteration (Fig. 5). The lack of any correlation also suggests minimal post-depositional diagenetic alteration. The higher amounts of Mn and Fe and occasional outliers displaying more negative $\delta^{18}O$ and $\delta^{13}C$ values (Figs 5 and 6) noted in some of the belemnites are regarded as an artefact of diagenetic alteration. Those samples where Fe concentrations were >150 ppm were considered likely to have undergone some isotopic exchange registered by the precipitation of post-depositional ferroan calcite and were excluded from any further analysis.

The oxygen and carbon isotope values of Volgian–early Hauterivian belemnites from Location One range from −2.26 to 1.25‰ and from −1.13 to 2.41‰, respectively (Fig. 3). The belemnites sampled from the succession of Volgian age were typical boreal species *Lagonibelus* cf. *elongates* and *Lagonibelus gustomesovi*. The presence of both species is consistent with the age determinations provided by ammonite data. Within the Ryazanian and Valanginian–early Hauterivian part of the succession, the belemnite species have been identified as dominated by *Cylindroteuthis* (*Arctoteuthis*) *subconoidea*, *Cylindroteuthis* (*Arctoteuthis*) cf. *repentina*, *Cylindroteuthis* (*Arctoteuthis*) cf. *porrectiformis*, *Acroteuthis explanatoides*, *Acroteuthis* (*Acroteuthis*) *paracmonoides arctica* and *Acroteuthis explorata*. Oxygen and carbon isotope ratios throughout the section show both short- and long-term variation. Oxygen isotope ratios fluctuate during the Volgian–early Valanginian interval and show relatively negative oxygen isotope ratios (*c*. −2.0‰), and by the early Valanginian the values become more positive (*c*. 0.0‰). Superimposed upon this trend, shorter-term more negative intervals are clearly recognized in the earliest Ryazanian and the earliest Valanginian intervals. In the upper part of the succession (*P. michalskii*–*H. bojarkensis* zones), more positive oxygen isotope values are seen, ranging from −0.82 to 1.25‰. The $\delta^{13}C_{carb}$ ratios generally rise from the lowest values (*c*. −1.15‰) in the late Volgian, before rising during the late Valanginian (*P. michalskii*–*H. bojarkensis* zone, Fig. 3), for which values range from 0.64 to 2.41‰. A plot of all $\delta^{18}O$ v. $\delta^{13}C$ data from this location (Fig. 6) reveals a significant positive correlation (at the 95% confidence level using a Student *t*-test).

The oxygen and carbon isotope values of Valanginian–Hauter-

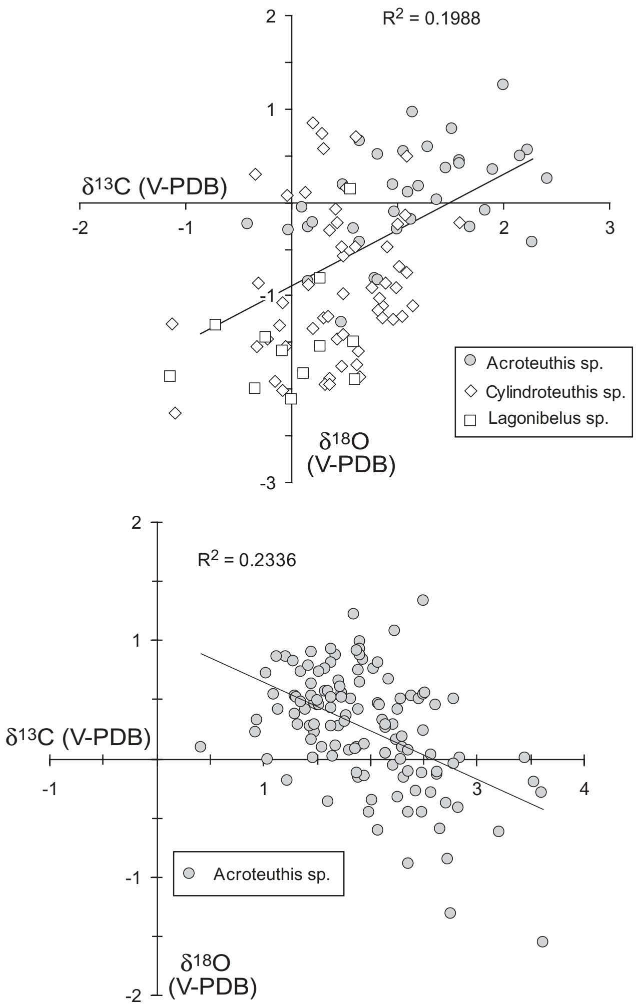

Fig. 6. Cross-plot of $\delta^{18}O$ and $\delta^{13}C$ values derived from belemnite samples of the Yatria River

ivian belemnites from Location Two range from −1.55 to 1.34‰ and from 0.41 to 3.62‰, respectively (Figs 4 and 6). The belemnites sampled from the succession consist of *Acroteuthis* (*A.*) *explanatoides*, *A.* (*Boreioteuthis*) *explorata*, *A.* (*B.*) cf. *anabarensis*, *A.* (*A.*) *paracmonoides arctica*, *A.* (*A.*) *hauthali*, *A.* (*A.*) *bojarcae* and *A.* (*A.*) *vnigri*. Although the data show a large amount of scatter, the most positive carbon isotope values are again observed in the *michalskii–ramulosus* ammonite zones. The oxygen and carbon isotope ratios through the section show a degree of symmetry. Increases in $\delta^{13}C$ are mirrored by decreases in $\delta^{18}O$ (Fig. 6). The plot of all $\delta^{18}O$ v. $\delta^{13}C$ data from this location reveals a significant negative correlation (at the 95% confidence level using a Student *t*-test).

Discussion

Palaeontological results

The belemnites observed in the Yatria River sections are clearly of Boreal–Arctic affinities and none of these taxa has ever been observed in Tethyan sediments of late Jurassic–early Cretaceous age. Whereas *Cylindroteuthis* and *Lagonibelus* are typical for the Oxfordian–Hauterivian of the Boreal–Arctic Province (Arctic, Siberia, western North America, Pechora Basin) they are absent from the Boreal–Atlantic Province (Russian Platform, eastern and NW Europe) from the Tithonian onward. *Acroteuthis* on the other hand is a Boreal–Atlantic genus, which migrated into the Boreal–Arctic Province only in the Berriasian. Evolution of endemic forms was widespread in the Tethyan and Boreal Realms, in Tithonian–Berriasian times, as a result of palaeobiogeographical isolation. It was the Valanginian sea-level rise (see Fig. 8), that allowed certain marine biota (e.g. coccoliths, ammonites) to attain gradually a more cosmopolitan distribution. As the distinctive provincialism of belemnites prevailed until the Barremian–Aptian, other factors (temperature, biology) may have played a role as well. Mutterlose & Kessels (2000) argued for cool polar conditions of the Berriasian and Valanginian in the Norwegian and Barents Sea, based on observations from calcareous nannofossils. The presence of bipolar floral belts in the high latitudes of the northern and southern hemisphere lend support to the idea of substantial temperature gradients (e.g. Crame 1993; but see also Hallam 1994). Thus temperature may explain the distinctive provincialism of belemnites. It is, however, also possible that the belemnite genera discussed here were relatively poor swimmers unable to cross larger areas of water. Sea level and climate are ultimately linked, and their effects cannot always be separated. Sea-level lowstands correspond to endemism, whereas highstands allow increasing exchange and promote more cosmopolitan assemblages.

The $\delta^{18}O$ record and palaeotemperature implications

Because of the combined effects of evaporation, precipitation, Rayleigh distillation and atmospheric vapour transport, seawater $\delta^{18}O$ compositions can vary by as much as 1.5‰ between low and high latitudes in the open ocean (Broecker 1989). Isotopically depleted water vapour is transported away from the subtropics towards the poles, elevating subtropical $\delta^{18}O_{seawater}$ compositions, and lowering high-latitude $\delta^{18}O_{seawater}$. Furthermore, because of the likely near proximity of a landmass (see Fig. 2), and hence the probable influence of riverine runoff and perhaps seasonal ice-melt, the seawater in this region may also have been characterized by a lower salinity and decreased $\delta^{18}O$ values. For example, Ekwurzel *et al.* (2001) and Polyak *et al.* (2003) showed that the $\delta^{18}O$ of water from the Arctic Ocean falls along a mixing line between Atlantic water ($\delta^{18}O$ 0.3 ± 0.1‰) and Arctic River runoff ($\delta^{18}O$ −18‰), giving Arctic Ocean waters a $\delta^{18}O$ range of *c.* 0.3 to −3.0‰. As the belemnite samples were derived from a marine system (based upon the presence of a fully marine fauna including ammonites), a riverine influence upon oxygen isotopes is, however, likely to be minimal. For example, Polyak *et al.* (2003) demonstrated that calcite precipitated within riverine-influenced waters of the modern Kara and Pechora Seas was likely to be characterized by negative (−3 to −5‰) carbon isotopes reflecting the combined effect of riverine dissolved inorganic carbon and organic remineralization. The carbon isotope data recorded in this study, as noted above, range from −1.13 to 3.62‰. Hence the observed isotopic variation is likely to be due to long-term temperature variation, although regional variation in $\delta^{18}O_{seawater}$ cannot be excluded (see below). The temperature–salinity plot shown in Figure 7, modified from Woo *et al.* (1992) after the model of Railsback *et al.* (1989), can be used to estimate the temperature range of the marine waters of the Yatria River area during the late Jurassic–early Cretaceous.

The Railsback *et al.* (1989) model assumes that the $\delta^{18}O$ of calcite precipitated in equilibrium with seawater is determined by

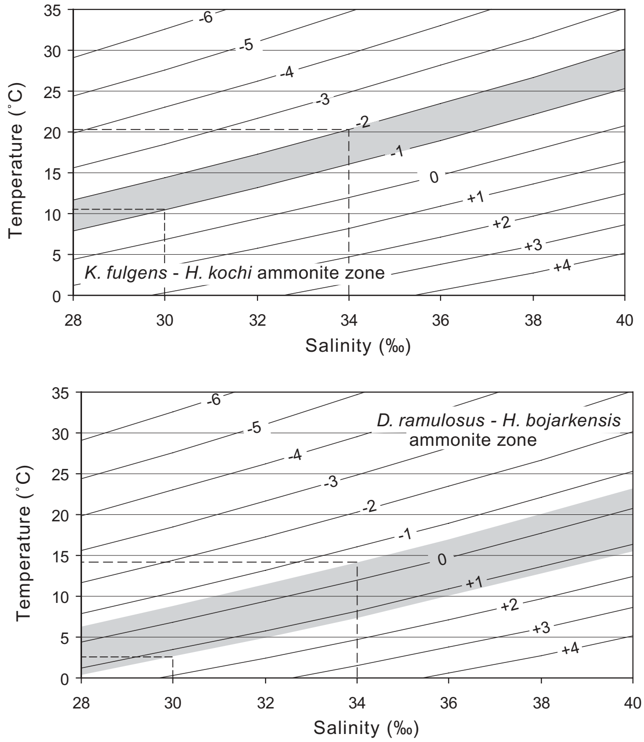

Fig. 7. Palaeotemperature estimates for the *K. fulgens–H. kochi* and *D. ramulosus–H. bojarkensis* ammonite zones. The plots are modified from Woo *et al*. (1992) after the model of Railsback *et al*. (1989) for an ice-free Earth with a seawater oxygen isotopic composition of −1‰ and mean salinity of seawater of 34.0‰. The continuous diagonal lines are isopleths of $\delta^{18}O$ values and show the possible combination of temperature (calculated using the equation of Anderson & Arthur 1983) and salinity that corresponds to calcite of a given isotopic composition and seawater. Explanation of shaded areas is given in the text.

a combination of seawater temperature and $\delta^{18}O_{seawater}$, which can be related to salinity. Thus minor variation in $\delta^{18}O_{seawater}$ can be incorporated into the calculations. The model assumes an ice-free Earth with a $\delta^{18}O_{seawater}$ composition of −1‰ and salinity of mean seawater of 34.0‰. The values used for salinity and oxygen isotopic composition are those calculated by Shackleton & Kennett (1975). The uncertainties in these values in the volume and $\delta^{18}O$ of ice are large enough to accommodate a modest volume of high-latitude ice during the Cretaceous (Woo *et al*. 1992). Each isopleth indicates the possible combination of temperature (calculated using the equation of Anderson & Arthur 1983) and salinity that corresponds to calcite of a given isotopic composition and seawater. For example within the model, a salinity value of 28‰ corresponds to a $\delta^{18}O_{seawater}$ value of *c*. −2.8‰, which is close to the observed value of the modern Arctic Ocean noted above. In an analysis of the transformation of ikaite to calcite from the Aptian high latitudes of Australia, De Lurio & Frakes (1999) provided a similar lower limit on the oxygen isotopic composition of the pore waters of −2.6 to −3.4‰.

The shaded areas in Figure 7 delineate the maximum range of oxygen isotopic values derived from the belemnites from two selected parts of the succession. Given the presence of a fully marine fauna, the salinity for the Yatria River area, within an ice-free Earth, is likely to have ranged within 'normal' marine conditions of *c*. 34.0‰ to *c*. 30‰, if the comparison between belemnites and modern cuttlefish (*Sepia officianalis*) has some validity. Although modern cuttlefish can survive in salinities as low as 20.0‰, the abundance and faunal diversity is greatest where salinity is >30‰ (e.g. von Boletzky 1999). Hence the oxygen isotopic data derived from the late Volgian *K. fulgens* to basal Ryazanian *H. kochi* ammonite zone ranging from −2.02 to −0.96‰, using the above limits of salinity, translate into a temperature range of 11–21 °C. Data from the late Valanginian–early Hauterivian *D. ramulosus–H. bojarkensis* zones from both locations reveal an almost identical range (the minimum and maximum values (−0.82 to 1.34‰) are plotted in Fig. 7). Using the same estimated salinity range provides a temperature range of 2–14 °C. It is of note that the study of Polyak *et al*. (2003) recorded a similar annual range of temperatures: −1 to +12 °C.

This analysis reveals that the highest palaeotemperatures are evident within the latest Volgian to earliest Ryazanian. Clearly, isotopic values become more positive in the upper part of the Ryazanian, before more negative values recur across the Ryazanian–Valanginian boundary, interpretable as a fall followed by a rise in palaeotemperatures (Fig. 7). The lowest temperatures, as outlined above, are encountered from the late Valanginian–early Hauterivian *P. michalskii–H. bojarkensis* zones. The development of low temperatures in these high-latitude regions provides adequate scope to argue for the presence of high-latitude ice and is consistent with the abundant glendonite occurrences of mid-Jurassic to early Cretaceous age described by Kaplan (1978) from slightly further north in the Taymyr peninsular region. A relatively cold Valanginian has also been proposed by Price *et al*. (2000), and by Ditchfield (1997), who suggested mean palaeotemperatures of 8.1 °C based on the isotopic analysis of endemic belemnites from Svalbard. Likewise, De Lurio & Frakes (1999), in a study reassessing belemnite-derived oxygen isotope palaeotemperatures from the Eromanga Basin, Australia, suggested Valanginian paleotemperatures ranging from −1 to 5 °C (which were previously reported as 11–16 °C) and within the ikaite stability temperature range.

The Paranà–Etendeka flood volcanism and associated intrusions are dated at 132 (± 1) Ma (Renne *et al*. 1996), coincident with the Valanginian–Hauterivian boundary. The primary isotopic imprint of volcanic CO_2 upon marine carbon isotope signatures is likely to have been small. Although relatively short-term cooling, particularly of terrestrial environments, is associated with volcanic SO_2 emissions, the Paranà–Etendeka flood volcanism would have also released large volumes of CO_2 into the atmosphere. The cumulative effects of successive large eruptions, typical of those encountered in flood basalt volcanism, could have therefore released sufficient CO_2 to cause significant longer-term greenhouse warming. Given that the most positive oxygen isotope data straddle the Valanginian–Hauterivian boundary, as noted above (Fig. 8), it would appear that there was either a decoupling of high-latitude temperatures from the intuitive response of volcanically induced climate warming, or alternatively CO_2 emissions from the Paranà–Etendeka flood volcanism were relatively low. A large temperature difference between the Atlantic–Tethys and Western Siberia–Arctic ocean could have in part resulted from the partial isolation of the Boreal Arctic Ocean from warmer Tethyan waters as a consequence of restricting marginal and intrabasinal highs. However, ocean temperatures inferred from the oxygen isotope compositions of fish teeth enamel, from the western Tethyan platform, also indicate a cooling event during the late Valanginian (*verrucosum–trinodosum* ammonite zones) (Pucéat *et al*. 2003). An increase in the relative abundance of boreal nannofossils in Romania during the late Valanginian (e.g. Melinte & Mutterlose 2001) also supports

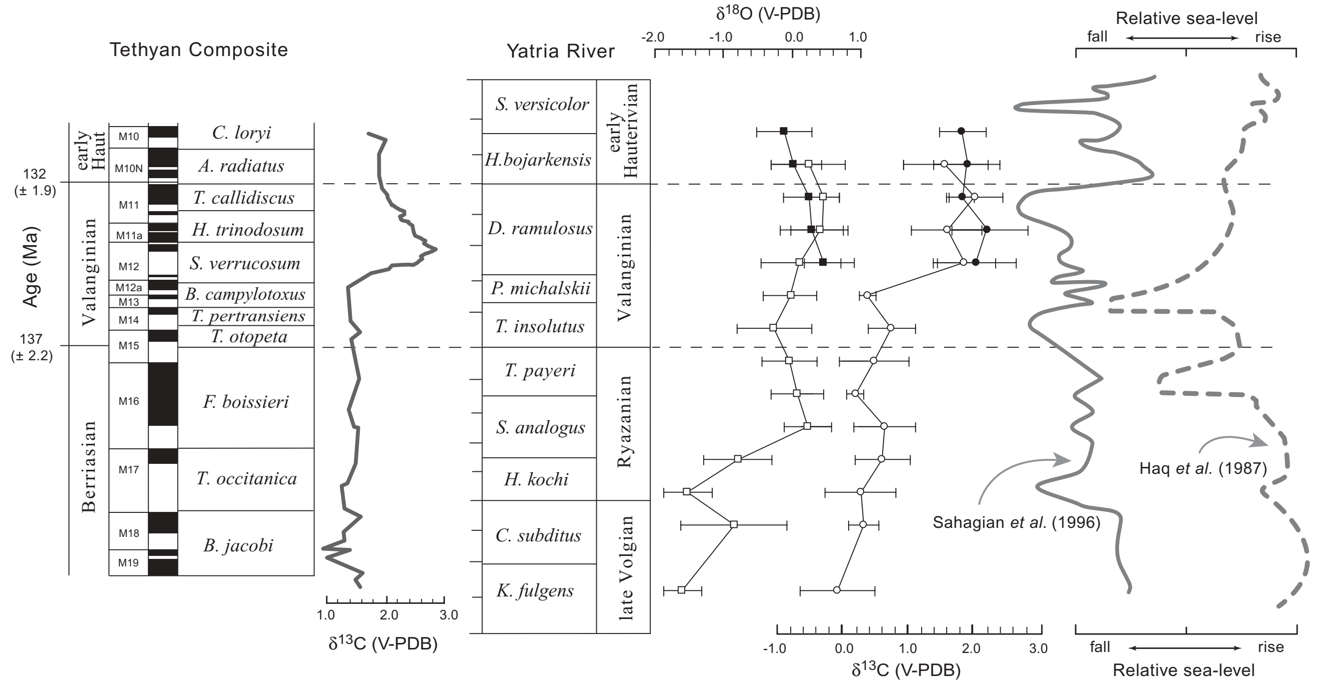

Fig. 8. A composite oxygen and carbon isotope curve for the late Volgian–early Hauterivian of the Yatria River. The data represent averages per million year period and show 1 SD. All data are calibrated against ammonite zones and/or the stage boundary ages assuming a constant sedimentation rate (ages from Gradstein *et al*. 1995). The filled symbols are from Location Two. The eustatic sea-level curves are from Haq *et al*. (1987) and Sahagian *et al*. (1996). The Tethyan composite carbon isotope stratigraphy and ammonite biostratigraphy data are from Weissert & Mohr (1996), Weissert *et al*. (1998) and van de Schootbrugge *et al*. (2000). Correlation between the Tethyan composite section and the Yatria River sections is based upon the ammonite correlations identified by Sahagian *et al*. (1996), Baraboshkin (2002) and Baraboshkin *et al*. (2003).

low temperatures within Tethys during this time. The lack of a warming response therefore during this interval may relate to the effectiveness of available carbon sinks and their ability to draw down atmospheric CO_2, moderating and stifling the effects of any volcanically induced greenhouse warming (see below). Certainly the positive carbon isotope excursion at this interval attests to either increased burial of organic carbon attributed to enhanced preservation under reduced O_2 conditions or changes in surface water productivity.

The $\delta^{13}C$ record

Published marine carbonate carbon isotope ($\delta^{13}C_{carb}$) records for the latest Jurassic–early Cretaceous have been constructed from outcrop exposures in northern Italy, France and Switzerland (e.g. Föllmi *et al*. 1994; Weissert & Mohr 1996; Weissert *et al*. 1998). The overall pattern of the marine record displays a period of decreasing carbon isotope values across the Jurassic–Cretaceous boundary, relatively stable $\delta^{13}C_{carb}$ values in the early Valanginian, then a rapid excursion to more positive values in the mid-Valanginian (*campylotoxus* zone), which subsequently return to pre-excursion values in the late Valanginian (*verrucosum–trinodosum* ammonite zones) (Fig. 8).

A positive carbon isotope excursion is also seen in the data from this study, beginning in the *P. michalskii* ammonite zone (correlatable with the *campylotoxus* zone). Previous concepts of marine carbon isotope ratios have generally associated rising sea levels with positive excursions, whereas negative excursions are usually associated with a fall in sea level (e.g. Arthur *et al*. 1988; Weissert & Lini 1991). The Valanginian positive carbon isotope excursion has been related directly to episodes of platform drowning within Tethys (e.g. Lini *et al*. 1992; Föllmi *et al*. 1994; Weissert *et al*. 1998). Positive carbon isotope excursions have also been attributed to increased burial of organic carbon either owing to enhanced preservation under reduced O_2 conditions (e.g. Bralower & Thierstein 1984) or driven by changes in surface water productivity. Models have been presented whereby the leaching of nutrients on coastal lowlands during a rise in sea level, possibly triggered by globally higher temperatures, resulted in increased ocean fertilization, productivity and an expansion of the oxygen minimum zone (e.g. Weissert 1989). As outlined by van de Schootbrugge *et al*. (2000), one of the difficulties associated with this model is that during the Hauterivian two or more phases of platform drowning are not mirrored by positive carbon isotope excursions, but instead a negative excursion or stable pattern. Wortmann & Weissert (2001) suggested that it is the transition to more positive values that coincides with a sea-level rise and a drowning of platform carbonates. As seen in Figure 8, the most positive carbon isotope values also coincide with a projected sea-level fall (using the data of Sahagian *et al*. (1996)). Although a late Valanginian regression is at odds with the sea-level curve of Haq *et al*. (1987), Baraboshkin *et al*. (2003) noted that during the late Valanginian the Russian Platform became even shallower, leading to complete isolation from Tethys. A number of studies do show that regressive systems are sometimes associated with positive carbon isotope excursions (e.g. Brenchley *et al*. 1994; Gröcke *et al*. 1999). An increased input of nutrients with a sea-level lowstand may arise from the exposure and erosion of a greater area of lowlands. The oxygen isotope data from this study clearly reveal that the most positive $\delta^{18}O$ values, indicative of the lowest temperatures, coincide with the most positive carbon isotope values. A possible mechanism to account for both positive $\delta^{13}C_{carb}$ values and low temperatures could be that the burial of large amounts of organic carbon-rich sediments depleted atmospheric CO_2 sufficiently to cause a significant drop in temperature (the 'Monterey Hypothesis' of Vincent & Berger (1985)). Such a scenario has been suggested for the Cenomanian–Turonian boundary event (Arthur *et al*. 1988) and for the mid-Miocene cooling (Vincent & Berger 1985). Evidence seems to indicate that the Cenomanian–Turonian burial event led to a 40–80% reduction in CO_2 levels (Kuypers *et al*. 1999), and may have caused a drop in temperature of the order of 10 °C in Europe (Arthur *et al*. 1988).

Evidence for widespread late Valanginian marine organic-rich black shales is, however, somewhat limited. Many Ocean Drilling Program (ODP) and Deep Sea Drilling Project (DSDP) sites in the Atlantic do contain organic-rich horizons of Valanginian age (e.g. Sites 416 and 638), although they are of dominantly terrestrial origin (e.g. Claypool & Baysinger 1980). DSDP Site 535 contains an interval with appreciable amounts of marine organic matter (Herbin *et al*. 1984), which is coincident with the Valanginian positive carbon isotope excursion (Lini *et al*. 1992). More recently, ODP Leg 198, drilled on Shatsky Rise in the West Pacific, recovered (at Site 1213) pelagic sequences containing two organic-rich intervals of marine origin from the Valanginian (Shipboard Scientific Party 2002). Tethyan successions of Valanginian age are also dominated by continental and amorphous organic matter, whereas only a minor component is derived from marine phytoplankton (e.g. Bersezio *et al*. 2002). The absence of widespread organic-rich black shale deposits of Valanginian age may be related to a number of factors: they may have been eroded (e.g. Weissert *et al*. 1998) or the burial of organic carbon might have occurred outside Tethys; for example, at high latitudes or outside typical marine settings. Northern hemisphere high-latitude basins with early Cretaceous organic-rich sediments possibly include Alaska (e.g. Magoon *et al*. 1999) or central Siberia (e.g. Peters *et al*. 1993; Baraboshkin *et al*. 2003). The partial separation of Tethyan and Boreal realms during sea-level lowstands (Fig. 8) in the Ryazanian and Valanginian could certainly have restricted ocean circulation (e.g. Gradstein *et al*. 1999; Mutterlose & Kessels 2000; Mutterlose *et al*. 2003) and potentially have enhanced discrete episodes of ocean stratification, promoting the deposition and preservation of organic carbon-rich marine sediments in these high-latitude areas. Undoubtedly the dynamics of high-latitude Jurassic–Cretaceous oceans remain poorly understood, in part related to the lack of modern analogues. In the Volgian and Hauterivian interval the ocean circulation pattern may have changed to a more vigorous ventilated pattern.

As noted above, the Valanginian positive carbon isotope excursion from Tethyan successions has been interpreted in terms of increased burial of organic carbon attributed to increased productivity brought about through upwelling or accelerated weathering and riverine nutrient transfer, increasing ocean fertilization (e.g. Föllmi *et al*. 1994; Weissert *et al*. 1998). In comparison with these relatively low-latitude settings, a number of pertinent differences exist at higher latitudes; for example, rates of weathering are much lower because of the prevalent cold climate and reduced rates of weathering in the sediment source area (e.g. Summerfield & Hulton 1994; Potter *et al*. 2001). The shift in mode from warmth in the Volgian to cooler climates in the late Valanginian–Hauterivian observed at Location One is independent of any observed changes in $\delta^{13}C$, whereas there is a degree of symmetry seen in the data from location Two. Increases in $\delta^{13}C$ are mirrored by decreases in $\delta^{18}O$ as evidenced by the cross-plots (Fig. 6). These relatively short-term trends appear therefore superimposed upon the longer-term patterns described above. The isotopic pattern may therefore be explainable by shorter-term pulses of increased productivity brought about by warming and periods of accelerated weathering and associated riverine nutrient transfer, and possibly the seasonal melting of ice releasing further nutrients (e.g. Smith & Nelson 1985; Wollenburg *et al*. 2001). These processes offer a conceivable explanation for the isotopic trends, whereby positive $\delta^{13}C$ values reflect increased productivity, whereas decreases in $\delta^{18}O$ relate to warming and possibly the input of isotopically depleted melt waters.

It has been suggested that in the absence of obvious 'global' marine black shales associated with positive $\delta^{13}C$ excursions (e.g. Shackleton 1987), burial of carbon may have occurred in terrestrial settings. Likewise, isotopic investigations have shown that early Cretaceous pelagic black-shale deposition does not necessarily coincide with positive carbon isotope values (e.g. Menegatti *et al*. 1998), and hence coupled changes in both the marine and terrestrial organic and carbonate flux may therefore contribute to excursions in the carbon isotope record (e.g. Weissert *et al*. 1998; Erba *et al*. 1999). Given the absence of widespread marine black shales of late Valanginian age so far identified, and because the most positive carbon isotope values are also coincident with a projected sea-level fall (Fig. 8), the possibility exists that during the Valanginian organic carbon was stored in terrestrial environments. A regression would have presumably resulted in the emergence of vast areas along the margins of the epicontinental seaways characterizing Europe and Siberia (Fig. 2), thus allowing lakes and coastal marshes to develop on newly formed coastal plains. Some models have suggested that coal is stored in paralic zones within both mid- and late lowstand and early and mid-highstand system tracts (e.g. Bohacs & Suter 1997).

Conclusions

The new isotopic data presented in this detailed study of Boreal belemnites from the latest Jurassic–early Cretaceous (Volgian–Valanginian) interval from the Yatria River reveal a shift to lower temperatures from the Volgian to the late Valanginian. Warmer phases are recognized within the late Volgian, earliest Ryazanian and earliest Valanginian. The lowest temperatures as outlined above are encountered from the late Valanginian–early Hauterivian *P. michalskii–H. bojarkensis* zones. The evidence points strongly to the conclusion that low ocean temperatures are consistent with limited polar ice and suggest that the region was at times considerably colder than previously thought. The observed distribution patterns of marine faunas across the Jurassic–Cretaceous boundary can be best explained though endemic evolution in the Tethyan and Boreal Realms, as a result of palaeobiogeographical isolation in Tithonian–Berriasian times. Because distinctive provincialism of belemnites prevailed until the Barremian–Aptian, other factors such as temperature may have also played an important role. Thus low polar temperatures and hence substantial temperature gradients may in part explain the observed distinctive provincialism of belemnites.

A positive shift in carbon isotope values during the late Valanginian is identified and considered correlatable with carbon isotope records from Tethyan successions. In the absence of an obvious 'global' marine black shale associated with the positive $\delta^{13}C$ excursion, burial of carbon may have occurred in terrestrial settings. Surprisingly, the most positive carbon isotope values correspond to the most positive oxygen isotope values (and hence lowest palaeotemperatures) and to a period characterized by inferred eustatic sea-level fall. This relationship, contrary to some models of carbon cycling, may indicate the effectiveness of available carbon sinks and their ability to draw down atmospheric CO_2, the 'inverse greenhouse' effect. The partial separation of Tethyan and Boreal realms during sea-level lowstands in the Ryazanian and Valanginian could have restricted ocean circulation and this is clearly indicated by the distinctive provincialism of marine biota for this interval, resulting in the absence of Tethyan elements in the Yatria River area or basin. Because of the prevalent cold climate, at these higher latitudes where rates of weathering were presumably much lower, pulses of productivity may be related not only to riverine nutrient transfer but also to melting of seasonal ice releasing further nutrients into the ocean.

This study was in part funded by a Royal Society Grant (to G.D.P.) and the Deutsche Forschungsgemeinschaft (Mu 667/19-1). We are grateful for the technical support provided by R. Bowers of the University of Plymouth and the assistance of E. Baraboshkin (Moscow State University). This paper benefited from the constructive reviews of S. Hesselbo and H. Weissert, and the editoral commments of A. Cohen.

References

Alley, N.F. & Frakes, L.A. 2003. First known Cretaceous glaciation: Livingston Tillite Member of the Cadna-owie Formation, South Australia. *Australian Journal of Earth Sciences*, **50**, 139–144.

Anderson, T.F. & Arthur, M.A. 1983. Stable isotopes of oxygen and carbon and their application to sedimentologic and environmental problems. *In:* Arthur, M.A., Anderson, T.F., Kaplan, I.R., Veizer, J. & Land, L.S. (eds) *Stable isotopes in Sedimentary Geology.* Society of Economic Paleontologists and Minerologists Short Course Notes, **10**, 1.1–1.151.

Arthur, M.A., Dean, W.E. & Pratt, L.M. 1988. Geochemical and climatic effects of increased marine organic carbon burial at the Cenomanian/Turonian boundary. *Nature*, **335**, 714–717.

Baraboshkin, E.J. 2002. Early Cretaceous Seaways of the Russian Platform and the problem of Boreal/Tethyan correlation. *In:* Michalík, J. (ed.) *Tethyan/ Boreal Cretaceous Correlation*. VEDA, Bratislava, 39–78.

Baraboshkin, E.Y., Alekseev, A.S. & Kopaevich, L.F. 2003. Cretaceous palaeogeography of the North-Eastern Peri-Tethys. *Palaeogeography, Palaeoclimatology, Palaeoecology*, **196**, 177–208.

Bartolini, A. 2003. Cretaceous radiolarian biochronology and carbon isotope stratigraphy of ODP Site 1149 (Northwestern Pacific, Nadezhda Basin). *In:* Ludden, J.N., Plank, T. & Escutia, C. (eds) *Proceedings of the Ocean Drilling Program, Scientific Results, 185*. Ms 185SR-011.

Bennett, M.R. & Doyle, P. 1996. Global cooling inferred from dropstones in the Cretaceous—fact or wishful thinking. *Terra Nova*, **8**, 182–185.

Bersezio, R., Erba, E., Gorza, M. & Riva, A. 2002. Berriasian–Aptian black shales of the Maiolica formation (Lombardian Basin, Southern Alps, Northern Italy): local to global events. *Palaeogeography, Palaeoclimatology, Palaeoecology*, **180**, 253–275.

Bohacs, K.M. & Suter, J. 1997. Sequence stratigraphic distribution of coaly rocks; fundamental controls and paralic examples. *AAPG Bulletin*, **81**, 1612–1639.

Bralower, T.J. & Thierstein, H.R. 1984. Low productivity and slow deep-water circulation in mid-Cretaceous oceans. *Geology*, **12**, 614–618.

Brenchley, P.J., Marshall, J.D. & Carden, G.A.F. et al. 1994. Bathymetric and isotopic evidence for a short-lived Late Ordovician glaciation in a greenhouse period. *Geology*, **22**, 295–298.

Broecker, W.S. 1989. The salinity contrast between the Atlantic and Pacific Oceans during glacial time. *Paleoceanography*, **4**, 207–212.

Claypool, G.E. & Baysinger, J.P. 1980. Analysis of organic matter in sediment cores from the Moroccan Basin, Deep Sea Drilling Project Sites 415 and 416. *In:* Stout, L.N., Worstell, P., Lancelot, Y. et al. (eds) *Initial Reports of the Deep Sea Drilling Project*. US Government Printing Office, Washington, DC, **50**, 605–608.

Crame, J.A. 1993. Bipolar molluscs and their evolutionary implications. *Journal of Biogeogegraphy*, **20**, 145–161.

De Lurio, J.L. & Frakes, L.A. 1999. Glendonites as a paleoenvironmental tool: implications for early Cretaceous high latitude climates in Australia. *Geochimica et Cosmochimica Acta*, **63**, 1039–1048.

Dhondt, A.V. 1992. Palaeogeographic distribution of Cretaceous Tethyan nonrudist bivalves. *In:* Kollmann, H.A. & Zapfe, H. (eds) *New Aspects on Tethyan Cretaceous Fossil Assemblages*. Österreichische Akademie de Wissenschaften, Schriftenreihe der Erdwissenschaftlichen Komissionen, **9**, 75–94.

Dickson, J.A.D. 1966. Carbonate identification and genesis as revealed by staining. *Journal of Sedimentary Petrology*, **36**, 491–505.

Ditchfield, P.W. 1997. High Northern palaeolatitude Jurassic–Cretaceous palaeotemperature variation: new data from Kong Karls Land, Svalbard. *Palaeogeography, Palaeoclimatology, Palaeoecology*, **130**, 163–175.

Doyle, P. 1987. Lower Jurassic–Lower Cetaceous belemnite biogeography and the development of the Mesozoic Boreal Realm. *Palaeogeography, Palaeoclimatology, Palaeoecology*, **61**, 237–254.

Erba, E., Channell, J.E.T. & Claps, M. et al. 1999. Integrated stratigraphy of the Cismon APTICORE (Southern Alps, Italy): a 'reference section' for the Barremian–Aptian interval at low latitudes. *Journal of Foraminiferal Research*, **29**, 371–391.

Ekwurzel, B., Schlosser, P., Mortlock, R.A., Fairbanks, R.G. & Swift, J.H. 2001. River runoff, sea ice meltwater and Pacific water distribution and mean residence times in the Arctic Ocean. *Journal of Geophysical Research*, **106**, 9075–9092.

Föllmi, K.B., Weissert, H., Bisping, M. & Funk, H. 1994. Phosphogenesis, carbon-isotope stratigraphy, and platform evolution along the Lower Cretaceous northern Tethyan margin. *Geological Society of America Bulletin*, **106**, 729–746.

Frakes, L.A. 1979. *Climates through Geologic Time*. Elsevier, Amsterdam.

Frakes, L.A. & Francis, J.E. 1988. A guide to Phanerozoic cold polar climates from high latitude ice-rafting in the Cretaceous. *Nature*, **333**, 547–549.

Gavshyn, V.M. & Zakharov, V.A. 1996. Geochemistry of the Upper Jurassic–Lower Cretaceous Bazhenov Formation, West Siberia. *Economic Geology*, **91**, 122–133.

Golbert, A.V., Zakharov, V.A., Klimova, I.G. & Romanova, E.E. 1975. Yatria River. *In:* Saks, V.N. (ed.) *The Jurassic–Cretaceous Boundary and the Berriasian Stage in the Boreal Realm*. Keter, Jerusalem, 56–65.

Gradstein, F.M., Agterberg, F.P., Ogg, J.G., Hardenbol, J., van Veen, P., Thierry, J. & Huang, Z. 1995. A Triassic, Jurassic and Cretaceous timescale. *In:* Berggren, W.A., Kent, D.V., Aubry, M.-P. & Hardenbol, J. (eds) *Geochronology, Time Scales and Stratigraphic Correlation*. SEPM Special Publications, **54**, 95–128.

Gradstein, F.M., Kaminski, M.A. & Agterberg, F.P. 1999. Biostratigraphy and paleoceanography of the Cretaceous seaway between Norway and Greenland. *Earth-Science Reviews*, **46**, 27–98.

Gröcke, D., Hesselbo, S.P. & Jenkyns, H.C. 1999. Carbon-isotope composition of Lower Cretaceous fossil wood: ocean–atmosphere chemistry and relation to sea-level change. *Geology*, **27**, 155–158.

Hallam, A. 1993. Jurassic climates as inferred from the sedimentary and fossil record. *Philosophical Transactions of the Royal Society of London, Series B*, **341**, 287–296.

Hallam, A. 1994. An Outline of Phanerozoic Biogeography. *Oxford Biogeography Series*, 10.

Haq, B.U., Hardenbohl, J. & Vail, P.R. 1987. Chronology of fluctuating sea levels since the Triassic. *Science*, **235**, 1156–1167.

Herbin, J.P., Deroo, G. & Roucache, J. et al. 1984. Organic geochemistry of lower Cretaceous sediments from Site 535, Leg 77: Florida Straits. *In:* Buffler, R.T. & Schlager, W. (eds) *Initial Reports of the Deep Sea Drilling Project, 29*. US Government Printing Office, Washington, DC, 459–474.

Herman, A.B. & Spicer, R.A. 1997. New quantitative palaeoclimate data for the Late Cretaceous Arctic: evidence for a warm polar ocean. *Palaeogeography, Palaeoclimatology, Palaeoecology*, **128**, 227–251.

Hoedemaeker, P.J. 1990. The Neocomian boundaries of the Tethyan Realm based on the distribution of ammonites. *Cretaceous Research*, **11**, 331–342.

Hoedemaeker, P.J. & Rawson, P.F. 2000. Report on the 5th International Workshop of the Lower Cretaceous Cephalopod Team (Vienna, 5 September 2000). *Cretaceous Research*, **21**, 857–860.

Huber, B.T. 1998. Tropical paradise at the Cretaceous poles? *Science*, **282**, 2199–2200.

Kaplan, M.E. 1978. Calcite pseudomorphoses in Jurassic and Lower Cretaceous deposits of the Northern Area of Eastern Siberia. *Geologiya i Geofizika*, **19**, 62–70.

Kemper, E. 1987. Das Klima der Kreide-Zeit. *Geologische Jahrbuch*, **A96**, 5–185.

Krylov, N. & Korzh, M. 1984. Upper Jurassic bituminous shales in western Siberia. *Sedimentary Geology*, **40**, 211–215.

Kuypers, M.M.M., Pancost, R. & Sinninghe Damsté, J.S. 1999. A large and abrupt fall in atmospheric CO_2 concentrations during Cretaceous times. *Nature*, **399**, 342–345.

Lebedeva, N.K. & Nikitenko, B.L. 1999. Dinoflagellate cysts and microforaminifera of the Lower Cretaceous Yatria River section, Subarctic Ural, NW Siberia (Russia). Biostratigraphy, palaeoenvironmental and palaeogeographic discussion. *Grana*, **38**, 134–143.

Lini, A., Weissert, H. & Erba, E. 1992. The Valanginian carbon isotope event: a first episode of greenhouse climate conditions during the Cretaceous. *Terra Nova*, **4**, 374–384.

Magoon, L.B., Bird, K.J. & Burruss, R.C. *et al.* 1999. Evaluation of hydrocarbon charge and timing using the petroleum system. *In: The Oil and Gas Resource Potential of the 1002 Area, Arctic National Wildlife Refuge, Alaska. ANWR Assessment Team*. US Geological Survey Open-File Report, **98-34**, 1–66.

Melinte, M. & Mutterlose, J. 2001. A Valanginian (Early Cretaceous) 'boreal nannoplankton excursion' in sections from Romania. *Marine Micropaleontology*, **43**, 1–25.

Menegatti, A.P., Weissert, H., Brown, R.S., Tyson, R.V., Farrimond, P., Strasser, A. & Caron, M. 1998. High-resolution $\delta^{13}C$ stratigraphy through the early Aptian 'Livello Selli' of the Alpine Tethys. *Paleoceanography*, **13**, 530–545.

Michalik, J. 1992. The structure and distribution of the European Cretaceous brachiopod assemblages with emphasis on the Tethyan fauna. *In:* Kollmann, H.A. & Zapfe, H. (eds) *New Aspects on Tethyan Cretaceous Fossil Assemblages*. Österreichische Akademie de Wissenschaften, Schriftenreihe der Erdwissenschaftlichen Komissionen, **9**, 57–74.

Mutterlose, J. 1988. Migration and evolution patterns in Upper Jurassic and Lower Cretaceous belemnites. *In:* Wiedmann, J. & Kullmann, J. (eds) *2nd International Cephalopod Symposium: Cephalopods: Present and Past, O. H. Schindewolf Symposium*. Schweitzerbart, Stuttgart, 525–537.

Mutterlose, J. 1992. Biostratigraphy and paleobiogeography of early Cretaceous calcareous nannofossils. *Cretaceous Research*, **13**, 167–189.

Mutterlose, J. & Kessels, K. 2000. Early Cretaceous calcareous nannofossils from high latitudes: implications for palaeobiogeography and palaeoclimate. *Palaeogeography, Palaeoclimatology, Palaeoecology*, **160**, 347–372.

Mutterlose, J., Brumsack, H. & Flogel, S. *et al.* 2003. The Greenland–Norwegian Seaway: a key area for understanding Late Jurassic to Early Cretaceous paleoenvironments. *Paleoceanography*, **18**, 1010.

Peters, K.E., Kontorovich, A.E., Moldowan, J.M., Andrusevich, V.E., Huizinga, B.J., Demaison, G.J. & Stasova, O.F. 1993. Geochemistry of selected oils and rocks from the central portion of the West Siberian Basin, Russia. *AAPG Bulletin*, **77**, 863–887.

Pinous, O.V., Sahagian, D.L., Shurygin, B.N. & Nikitenko, B.L. 1999. High-resolution sequence stratigraphy and sea-level interpretation of the middle and upper Jurassic strata of the Nyurolskaya Depression and vicinity (southeastern West Siberia, Russia). *Marine and Petroleum Geology*, **16**, 245–257.

Pinous, O.V., Levchuk, M.A. & Sahagian, D.L. 2001. Regional synthesis of the productive Neocomian complex of West Siberia: sequence stratigraphic framework. *AAPG Bulletin*, **10**, 1713–1730.

Pirrie, D. & Marshall, J.D. 1990. High-paleolatitude Late Cretaceous paleotemperatures—new data from James Ross Island, Antarctica. *Geology*, **18**, 31–34.

Podlaha, O.G., Mutterlose, J. & Veizer, J. 1998. Preservation of $\delta^{18}O$ and $\delta^{13}C$ in belemnite rostra from the Jurassic/Early Cretaceous successions. *American Journal of Science*, **298**, 324–347.

Polyak, L., Stanovoy, V. & Lubinski, D.J. 2003. Stable isotopes in benthic foraminiferal calcite from a river-influenced Arctic marine environment, Kara and Pechora Seas. *Paleoceanography*, **18**, 1003.

Potter, P.E., Huh, Y. & Edmond, J.M. 2001. Deep-freeze petrology of Lena River sand, Siberia. *Geology*, **29**, 999–1002.

Price, G.D. 1999. The evidence and implications of polar-ice during the Mesozoic. *Earth-Science Reviews*, **48**, 183–210.

Price, G.D., Ruffell, A.H., Jones, C.E., Kalin, R.M. & Mutterlose, J. 2000. Isotopic evidence for temperature variation during the early Cretaceous (late Ryazanian–mid Hauterivian). *Journal of the Geological Society, London*, **157**, 335–343.

Pucéat, E., Lécuyer, C., Sheppard, S.M.F., Dromart, G., Reboulet, A. & Grandjean, P. 2003. Thermal evolution of Cretaceous Tethyan marine waters inferred from oxygen isotope composition of fish tooth enamels. *Paleoceanography*, **18**, 1029.

Railsback, L.B., Anderson, T.F., Ackerly, S.C. & Cisne, J.L. 1989. Paleoceanographic modeling of temperature–salinity profiles from stable isotope data. *Paleoceanography*, **4**, 585–591.

Rawson, P.F. 1994. Sea-level changes and their influence on ammonite biogeography in the European Early Cretaceous. *Palaeopelagos Special Publications*, **1**, 317–326.

Renne, P.R., Glen, J.M., Milner, S.C. & Duncan, A.R. 1996. Age of Etendeka flood volcanism and associated intrusions in southwestern Africa. *Geology*, **24**, 659–662.

Ruffell, A.H., Price, G.D., Mutterlose, J., Kessels, K., Baraboshkin, E. & Gröcke, D.R. 2002. Palaeoclimate indicators (clay minerals, calcareous nannofossils, stable isotopes) compared from two successions in the late Jurassic of the Volga Basin (SE Russia). *Geological Journal*, **37**, 17–33.

Sahagian, D., Pinous, O., Olferiev, A. & Zakharov, V. 1996. Eustatic curve for the Middle Jurassic–Cretaceous based on Russian platform and Siberian stratigraphy: zonal resolution. *AAPG Bulletin*, **80**, 1433–1458.

Shackleton, N.J. 1987. The carbon isotope record of the Cenozoic: history of organic carbon burial and of oxygen in the ocean and atmosphere. *In:* Brooks, J. & Fleet, A.J. (eds) *Marine Petroleum Source Rocks*. Geological Society, London, Special Publications, **26**, 423–434.

Shackleton, N.J. & Kennett, J.P. *et al.* 1975. Paleotemperature history of the Cenozoic and the initiation of Antarctic glaciation: oxygen and carbon isotope analyses in DSDP sites 277, 279 and 281. *In:* Kennett, J.P. & Houtz, R.E. (eds) *Initial Reports of the Deep Sea Drilling Project, 29*. US Government Printing Office, Washington, DC, 743–756.

Shipboard Scientific Party *et al.* 2002. Leg 198 summary. *In:* Bralower, T.J., Premoli Silva, I. & Malone, M.J. (eds) *Proceedings of the Ocean Drilling Program, Initial Reports, 198*. Ocean Drilling Program, College Station, TX, 1–148.

Smith, A.G., Smith, D.G. & Funnell, B.M. 1994. *Atlas of Mesozoic and Cenozoic Coastlines*. Cambridge University Press, Cambridge.

Smith, W.O. & Nelson, D.M. 1985. Phytoplankton bloom produced by a receding ice edge in the Ross Sea—spatial coherence with the density field. *Science*, **227**, 163–166.

Street, C. & Bown, P.R. 2000. Palaeobiogeography of Early Cretaceous (Berriasian–Barremian) calcareous nannoplankton. *Marine Micropaleontology*, **39**, 265–291.

Summerfield, M.A. & Hulton, N.J. 1994. Natural controls of fluvial denudation rates in major world drainage basins. *Journal of Geophysical Research*, **99**, 13871–13883.

van de Schootbrugge, B., Föllmi, K.B., Bulot, L.G. & Burns, S.J. 2000. Paleoceanographic changes during the early Cretaceous (Valanginian–Hauterivian): evidence from oxygen and carbon stable isotopes. *Earth and Planetary Science Letters*, **181**, 15–31.

Vincent, E. & Berger, W.H. 1985. Carbon dioxide and polar cooling in the Miocene: the Monterey Hypothesis. *In:* Sundquist, E.T. & Broecker, W.S. (eds) *The Carbon Cycle and Atmospheric CO_2: Natural Variations Archean to Present*. American Geophysical Union, Monograph, **32**, 455–469.

von Boletzky, S. 1999. Biology and biogeography of extant cephalopods. *Bulletin de la Société Géologique de France*, **170**, 205–215.

Weissert, H. 1989. C-isotope stratigraphy, a monitor of palaeoenvironmental change: a case study from the early Cretaceous. *Surveys in Geophysics*, **10**, 1–161.

Weissert, H. & Lini, A. 1991. Ice Age interludes during the time of Cretaceous greenhouse climate? *In:* Mueller, D.W., McKenzie, J.A. & Weissert, H. (eds) *Controversies in Modern Geology*. Academic Press, London, 173–191.

Weissert, H. & Mohr, H. 1996. Late Jurassic climate and its impact on carbon cycling. *Palaeogeography, Palaeoclimatology, Palaeoecology*, **122**, 27–43.

Weissert, H., Lini, A., Föllmi, K.B. & Kuhn, O. 1998. Correlation of Early Cretaceous carbon isotope stratigraphy and platform drowning events: a possible link? *Palaeogeography, Palaeoclimatology, Palaeoecology*, **137**, 189–203.

Wollenburg, J.E., Kuhnt, W. & Mackensen, A. 2001. Changes in Arctic Ocean paleoproductivity and hydrography during the last 145 kyr: the benthic foraminiferal record. *Paleoceanography*, **16**, 65–77.

Woo, K.-S., Anderson, T.F., Railsback, L.B. & Sandberg, P.A. 1992. Oxygen isotope evidence for high-salinity surface seawater in the Mid-Cretaceous Gulf of Mexico: implications for warm, saline deepwater formation. *Paleoceanography*, **7**, 673–685.

Wortmann, U.G. & Weissert, H. 2001. Tying platform drowning to perturbations of the global carbon cycle with a $^{13}C_{org}$-curve from the Valanginian of DSDP Site 416. *Terra Nova*, **12**, 289–294.

Zakharov, V.A., Bogomolov, Y.I. & Ilyina, V.I. *et al.* 1997. Boreal zonal standard and biostratigraphy of the Siberian Mesozoic. *Geologiya i Geofizika*, **38**, 927–956 (in Russian).

Received 5 November 2003; revised typescript accepted 10 May 2004.
Scientific editing by Anthony Cohen